Title

Unexpected Differences between Two Closely Related Bacterial P450 Camphor Monooxygenases.

Journal

Biochemistry, 59(29)

Authors

Murarka, Vidhi
Batabyal, Dipanwita
Amaya, Jose
et al.

Publication Date

2020-07-28

DOI

10.1021/acs.biochem.0c00366

Peer reviewed

HHS Public Access

Author manuscript

Biochemistry. Author manuscript; available in PMC 2021 July 28.

Published in final edited form as:

Biochemistry. 2020 July 28; 59(29): 2743–2750. doi:10.1021/acs.biochem.0c00366.

Unexpected Differences between Two Closely Related Bacterial P450 Camphor Monooxygenases

Vidhi C. Murarka,
Departments of Molecular Biology and Biochemistry, Pharmaceutical Sciences, and Chemistry, University of California, Irvine, California 92697-3900, United States

Dipanwita Batabyal,
Departments of Molecular Biology and Biochemistry, Pharmaceutical Sciences, and Chemistry, University of California, Irvine, California 92697-3900, United States

Jose A. Amaya,
Departments of Molecular Biology and Biochemistry, Pharmaceutical Sciences, and Chemistry, University of California, Irvine, California 92697-3900, United States

Irina F. Sevrioukova,
Departments of Molecular Biology and Biochemistry, Pharmaceutical Sciences, and Chemistry, University of California, Irvine, California 92697-3900, United States

Thomas L. Poulos
Departments of Molecular Biology and Biochemistry, Pharmaceutical Sciences, and Chemistry, University of California, Irvine, California 92697-3900, United States

Abstract

The bacterial cytochrome P450cam catalyzes the oxidation of camphor to 5-*exo*-hydroxycamphor as the first step in the oxidative assimilation of camphor as a carbon/energy source. CYP101D1 is another bacterial P450 that catalyzes the same reaction. A third P450 (P450tcu) has recently been discovered that has ≈86% sequence identity to P450cam as well as very similar enzymatic properties. P450tcu, however, exhibits three unusual features not found in P450cam. First, we observe product in at least two orientations in the X-ray structure that indicates that, unlike the case for P450cam, X-ray-generated reducing equivalents can drive substrate hydroxylation *in crystallo*. We postulate, on the basis of molecular dynamics simulations, that greater flexibility in P450tcu enables easier access of protons to the active site and, together with X-ray driven reduction, results in O_2 activation and substrate hydroxylation. Second, the characteristic low-spin

Corresponding Author: **Thomas L. Poulos** − Departments of Molecular Biology and Biochemistry, Pharmaceutical Sciences, and Chemistry, University of California, Irvine, California 92697-3900, United States; poulos@uci.edu.

The authors declare no competing financial interest.

Supporting Information

The Supporting Information is available free of charge at https://pubs.acs.org/doi/10.1021/acs.biochem.0c00366.

Sequence alignments (Figure S1), time-dependent spin shifts (Figure S2), molecular models (Figure S3), and crystallographic data collection and refinement statistics (Table S1) (PDF)

Accession Codes

Coordinates and structure factors have been deposited in the Protein Data Bank as entry 6WPL.

Complete contact information is available at: https://pubs.acs.org/doi/10.1021/acs.biochem.0c00366

to high-spin transition when camphor binds occurs immediately with P450cam but is very slow in P450tcu. Third, isothermal titration calorimetry shows that in P450cam substrate binding is entropically driven with a ΔH of >0 while in P450tcu with a ΔH of <0 with a more modest change in $-T\Delta S$. These results indicate that despite nearly identical structures and enzymatic properties, these two P450s exhibit quite different properties most likely related to differences in conformational dynamics.

Graphical Abstract

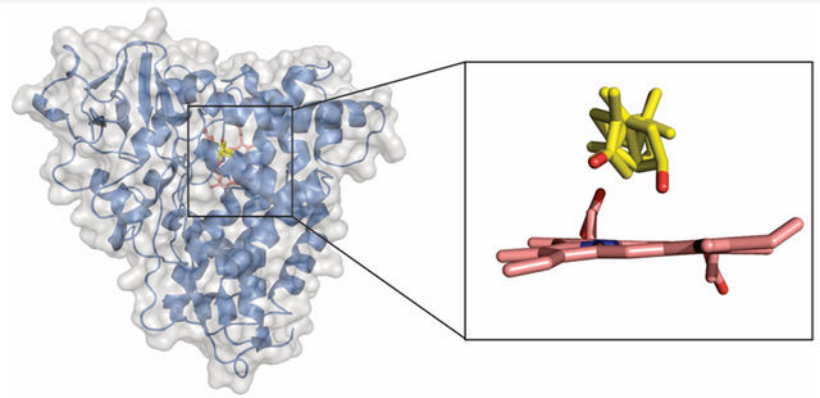

Cytochromes P450 are best known for catalyzing the oxidation of unactivated C–H bonds to give the corresponding alcohol.[1] The most well-studied P450 is CYP101A1 (P450cam) that catalyzes the oxidation of camphor to 5-*exo*-hydroxycamphor, the first step in the oxidative assimilation of camphor as an energy/carbon source in *Pseudomonas putida*. While serving as a paradigm for understanding the structural and mechanistic properties of P450s, P450cam exhibits certain mechanistic features that are not shared by many other P450s. The most important is the strict requirement for its own Fe_2S_2 ferredoxin redox partner, putidaredoxin (Pdx), in the second electron transfer.[2] Many P450s, but not P450cam, can utilize foreign redox partners as donors of the second electron. We now know that Pdx plays an “effector” role by binding to P450cam and switching the enzyme to a more open conformation[3–6] that establishes the proton relay network required for O_2 activation.[4] This level of specificity for a protein redox partner, however, is not shared by other camphor monooxygenases. For example, CYP101D1 catalyzes exactly the same reaction as P450cam with a similar rate and coupling efficiency, but unlike P450cam, it can utilize foreign redox partners.[7,8]

Structural differences around the critical active site Asp residue required in the O_2 activation proton relay network help to explain this difference. In P450cam, the critical Asp (Asp251) is tied up via salt bridges to Lys178 and Arg186 residues (Figure 1). The binding of Pdx results in structural changes that break these salt bridges, thereby freeing Asp251 to serve its catalytic function. In CYP101D1, Lys178 is replaced with Gly180 and the critical Asp259 is ion paired with only Arg188. In addition, Asp259 in CYP101D1 occupies two conformations.[7] The one fewer salt bridge and multiple conformations indicate that Asp259 is not as rigidly held in place as P450cam Asp251, and as a result, binding of a specific redox partner is not required for establishing the proton relay network in CYP101D1.

Recently, a third camphor monooxygenase has been discovered in *Pseudomonas* sp. strain TCU-HL1, which utilizes borneol as an energy/carbon source.[9] The first step in the assimilation of borneol is its oxidation to camphor and, subsequently, to 5-*exo*-hydroxycamphor by a P450cam-like monooxygenase, which we termed "P450tcu". Tsang et al. showed that *Pseudomonas* sp. has the genes that encode a P450cam-like camphor oxidation system, including the camC gene (THL1_4171 UniProt gene sequence) that encodes a P450.[9] Amino acid sequence comparisons (Figure S1) show that P450cam shares ≈86% identity with P450tcu but only 45% with CYP101D1. Given that CYP101D1 and P450cam exhibit quite different properties, we undertook this comparative study to investigate enzymatic behaviors of P450cam and P450tcu to better understand structure-function relationships in camphor monooxygenases. Here we present structural, enzymatic, and biochemical characterizations of P450tcu.

MATERIALS AND METHODS

Protein Expression and Purification.

Gene sequences that encode P450tcu and Pdxtcu were obtained from the UniProt database. Synthetic genes encoding these two proteins were codon optimized for expression in *Escherichia coli* (GeneScript, Inc.). The P450tcu gene was subcloned into pET28a (NdeI and BamI) with a thrombin-cleavable N-terminal six-His tag. The Pdxtcu gene was subcloned into pET17b (NdeI and EcoRI). Both plasmids were transformed into *E. coli* BL21(DE3) cells separately.

For P450tcu, transformed cells were grown in 1 L of Luria-Bertani (LB) broth containing kanamycin at 37 °C. When the culture reached an OD_{600} of 0.8–1.0, the temperature was decreased to 25 °C and the cells were induced with 1 mM isopropyl 1-thio-D-galactopyranoside. Sixteen hours after induction, cells were harvested by centrifugation and cell pellets were resuspended in lysis buffer containing 50 mM KP_i (pH 7.4) and 100 mM sodium chloride. This was followed by sonication and centrifugation at 4 °C. The supernatant was loaded on a Ni-IMAC column. The column was washed with lysis buffer containing 40 mM imidazole. Elution buffer containing 50 mM KP_i (pH 7.4) and 200 mM imidazole was used to elute the protein. The eluted protein was mixed with thrombin (20 units of thrombin/mg of P450tcu) to cleave the His tag and then dialyzed overnight against 50 mM KP_i (pH 7.4) at 4 °C. After dialysis, ammonium sulfate was added to reach 32% saturation and the solution was centrifuged at 14000 rpm for 1 h at 4 °C. The supernatant was loaded on a phenyl sepharose column, and protein was eluted with a 32% to 0% gradient of ammonium sulfate. The protein fractions were pooled, concentrated, and passed through a gel filtration Superdex 75 column equilibrated in 50 mM KP_i (pH 7.4) to achieve better purity.

Cells transformed with the Pdxtcu plasmid were grown in 1 L of LB medium containing ampicillin at 37 °C. The temperature was decreased to 25 °C when the OD_{600} reached 1. Cells were harvested after 40 h, and cell pellets were resuspended in lysis buffer containing 10 mM KP_i (pH 7.4) and 1 mM DTT. After sonication and centrifugation at 4 °C, the supernatant was loaded on a Q-sepharose column and washed with lysis buffer. The protein was eluted using a linear gradient from 0 to 500 mM KCl in 50 mM KP_i (pH 7.4) and 1 mM

DTT. The protein fractions were pooled, concentrated, and further purified on a Sephacryl S-200 HR column using 50 mM KP_i and 1 mM DTT as the buffer. Putidaredoxin reductase (Pdr) was expressed and purified using a previously published protocol.[10]

Enzyme Assays.

Camphor hydroxylation activity was determined by measuring NADH oxidation[11] at 25 °C by monitoring the change in absorbance at 340 nm with an extinction coefficient of 6.22 mM^{-1} cm^{-1}. The initial mixture consisted of 0.5 μM P450tcu, 5 μM Pdxtcu, 0.5 μM Pdr, and 200 μM NADH in 50 mM KP_i (pH 7.4). Reactions were initiated by the addition of 200 μM D-camphor. The NADH oxidation rate was determined as the difference in the rate before and after the addition of D-camphor.

The coupling efficiency in P450 reactions is the ratio of NADH oxidized to product formed. In a 100% coupled P450 system, one NADH molecule is oxidized per product molecule formed. To determine the coupling efficiency, the reaction was allowed to proceed such that a known amount of NADH was oxidized. After the completion of the reaction, 0.5 mM cineole was added as an internal standard, and the mixture was subjected to organic extraction using dichloromethane. This organic layer was then analyzed by GC-MS to estimate product formation.[12]

Isothermal Titration Calorimetry.

All experiments were performed on a MicroCal PEAQ-ITC instrument using a previously published protocol.[13] The concentration of substrate-free and substrate-bound P450tcu was measured using an ε_{418} of 115 mM^{-1} cm^{-1} and an ε_{392} of 100 mM^{-1} cm^{-1}, respectively. The Pdxtcu concentration was measured at 455 nm using an extinction coefficient of 5.9 mM^{-1} cm^{-1}.

Oxy Complex Stability.

The stability of the oxy-P450tcu complex was determined at 23 °C by stopped flow spectroscopy using an Applied Photophysics SX.18MV instrument. The buffer used in these experiments contained 50 mM KP_i (pH 7.4) and 1 mM D-camphor. P450tcu was degassed and purged with nitrogen, followed by reduction with a minimal amount of sodium dithionite. Reduced P450tcu was mixed in a 1:1 (v:v) ratio against oxygen-purged buffer in the absence and presence of a 2-fold excess of oxidized Pdxtcu to observe the formation and decay of the oxy complex. The concentrations of P450tcu and Pdxtcu before mixing were 9 and 18 μM, respectively.

Crystallization.

The hanging drop vapor diffusion method was used to grow P450tcu crystals. The reservoir solution contained 50–100 mM Bis-Tris (pH 6.5), 100 mM $MgCl_2 \cdot 6H_2O$, and 15–20% (w/v) PEG 3350. Drops (2 μL) of 20 mg/mL P450tcu [in 50 mM KP_i (pH 7.4) with 1 mM D-camphor] were mixed with 2 μL drops of the reservoir solution and equilibrated against 500 μL of the reservoir solution at room temperature. The crystals were flash-frozen using liquid nitrogen with ParatoneN (Hampton Research) as a cryoprotectant. Diffraction data were collected at the Stanford Synchrotron Radiation Lightsource beamline 12–2. MOSFLM[14] or

XDS[15] was used to index and integrate the raw data, and Aimless[16] used for scaling. The structure was determined by molecular replacement with Phaser[17] and P450cam as a search model (Protein Data Bank entry 5CP4). Phenix was used to carry out further refinements.[18] A summary of crystallographic statistics is provided in Table S1.

Computational Methods.

Molecular dynamics (MD) simulations were carried out with Amber 16 and 18. Details of the parameters and force field used were previously described.[19,20] Because the structure of P450tcu has a product in the active site, we placed a substrate molecule in the same location as the product for the MD simulations. Crystallographic waters were retained. Each structure was solvated in a rectangular box of TIP3P waters with a 10 Å cushion and Na^+ ions to maintain net neutrality. A total of ten 100 ns production runs were carried out for both structures with each 100 ns run using a different starting velocity. Snapshots were saved every 20 ps giving a total of 50000 snapshots for further analyses using *cpptraj*.[21]

RESULTS

Substrate and Redox Partner Binding.

Camphor binding results in a low-spin to high-spin spectral change in both P450cam and P450tcu. However, the high-spin transition in P450cam occurs immediately upon camphor addition but is very slow with a half-life of 25 min (Figure S2) in P450tcu. This indicates that P450tcu undergoes a very slow structural change required to switch the heme from low- to high-spin. Association of camphor with P450cam was previously measured by isothermal titration calorimetry (ITC), which showed that this process is entropically driven ($\Delta H > 0$).[13] With P450tcu, camphor binding gave the opposite result, with a ΔH of <0 (Figure 2 and Table 1). Despite this difference, the ΔG values of binding derived from the obvious thermograms are similar (Table 1).

ITC can also be used to investigate redox partner interactions. Previously, we demonstrated that Pdx binds more tightly to substrate-free P450cam,[22] which is consistent with the notion that Pdx shifts P450cam toward the more open low-spin state. As shown in Figure 3, Pdxtcu also binds more tightly to substrate-free P450tcu. Another important feature is the destabilizing effect of Pdx on the ferrous P450cam-dioxygen (P450cam-oxy) complex. The P450cam–oxy complex is quite stable ($t_{1/2}$ = 25 min) at 4 °C, yet its stability decreases by ~150-fold when oxidized Pdx is bound.[23] Pdxtcu has a similar effect and increases the decay of the P450tcu-oxy complex by ~140-fold at 23 °C (Figure 4). Again, this finding suggests Pdxtcu shifts P450tcu to a more open state that, in the absence of electron transfer, exposes the oxy complex to bulk solvent and disrupts the local stabilizing H-bonding network. In summary, the effect of Pdxtcu on P450tcu closely parallels what was observed with the P450cam–Pdx complex and suggests that oxidized Pdxtcu binds more tightly to substrate-free P450tcu and destabilizes the P450tcu-oxy complex.

Enzymatic Characterization.

In Table 2, we compare enzymatic activities of P450tcu and P450cam. The coupling efficiency is the ratio of NADH oxidized to product molecule formed. In a fully coupled

P450 reaction, 100% of NADH-derived electrons are utilized for the substrate oxidation, with one NADH molecule required for one product molecule formed.

As shown in Table 2, the P450tcu and P450cam monooxygenase systems have similar camphor oxidase activities (624 and 913 min^{-1}, respectively) and coupling efficiency (~95%). We also tested the ability of non-natural redox partners to support P450tcu catalysis. The CYP101D1 redox partner, Arx, cannot support P450cam or P450tcu catalysis. In contrast, the P450cam redox partner, putidaredoxin (Pdx), supports P450tcu and Pdxtcu, the ferredoxin from the P450tcu system, supports P450cam catalysis. Moreover, as shown previously for P450cam,[24,25] removal of the C-terminal Trp106 eliminates P450tcu activity. As noted earlier, Pdx plays an essential effector role in P450cam by shifting P450cam to a more open state that triggers the formation of a proton relay network required for O_2 activation.[4] Trp106 provides important nonbonded contacts with P450cam that favor the more open conformation.[4] Given the similarity of P450tcu and P450cam in redox partner selectivity, and the importance of Pdx Trp106 for functional activity, it is very likely that binding of Pdxtcu to P450tcu results in structural changes similar to those observed for P450cam redox partner binding.

Crystal Structure of P450tcu.

Sequence comparisons among three camphor monooxygenase (P450cam, P450tcu, and CYP101D1) are shown in Figure S1. Given the 86% sequence identity between P450cam and P450tcu, it is not surprising that the 2.1 Å crystal structure of P450tcu (Table S1) is very similar to the P450cam structure with a root-mean-square deviation among the Cα atoms of ~0.36 Å. Figure S3 highlights the location of sequence differences. Differences are scattered throughout the molecule and located primarily on the surface of the protein with no differences in the active site near the substrate (Figure S3). The closest difference to the active site is ≈11 Å from the camphor. There was, however, one striking difference. In camphor-bound P450cam, the substrate is well-ordered, with no signs of product formation. In P450tcu, the bound ligand is partially disordered, and the fitting indicates that it is a product, hydroxycamphor, rather than the substrate, camphor. Moreover, as shown in Figure 5, the product can fit into the electron density in two different orientations. In the first one, the product hydroxyl group extends down toward the iron, which is very similar to what was observed when P450cam crystals were soaked with the product.[26] However, when modeled in this substrate-like orientation, the extra density clearly indicates at least one additional orientation. This undoubtedly means that hydrated electrons, generated by the synchrotron X-ray beam, can drive substrate hydroxylation in P450tcu but not in wild type P450cam.

The product has been observed in WT P450cam in the P450–Pdx complex, where P450cam is locked in the open conformation,[4] and in a P450cam mutant where an ion pair to the essential Asp251 is disrupted.[13] Upon the Pdx-induced shift to a more open conformation, the Asp251-mediated salt bridges in P450cam are broken, thereby enabling solvent protons to protonate the iron-linked O_2 molecule.[13] P450tcu has the same set of salt bridges, and there is no obvious structural basis for these salt bridges to be weaker than in P450cam (Figure 1). We therefore turned to MD simulations to probe possible dynamical difference between P450tcu and P450cam that are not evident in crystal structures.

Molecular Dynamics.

Each P450 was subjected to ten 100 ns MD simulations using the same energy-minimized starting structures but different starting velocities. The overall relative flexibility can be assessed by examining temperature or B factors of Cα atoms. The only regions of substantial difference are located in surface loop regions. More revealing are the computed B factors of key regions of the active site. As shown in Table 3, camphor, Tyr96, and Asp251 all have much larger B factors in P450tcu than in P450cam. In addition, the H-bond between Tyr96 and the camphor carbonyl O atom is more stable in P450cam. In the ten 100 ns MD runs (a total of 50000 snapshots), the distance between the Tyr96 hydroxyl group and camphor carbonyl oxygen atom remains <3.0 Å 89% of the time, while in P450tcu, it is shorter than this distance only 62% of the time. Greater flexibility also is reflected in the crystallographic B factors. In P450tcu, the average side chain B factors for Tyr96 and Asp251 are 53% and 21%, respectively, higher than the average B factor for all Cα atoms. In P450cam, the average B factor is within 2% of being the same as Cα atoms for Asp251 while for Tyr96 it is ~15% lower. This greater dynamic flexibility in P450tcu is consistent with easier access of protons to the active site, which results in O_2 activation and substrate hydroxylation in P450tcu but not in P450cam. We also employed Mole2 (https://mol.upol.cz/), which computationally locates channels and pores in protein structures. As shown in Figure 6, P450cam and P450tcu display substantial differences in channels that connect the active site to the surface of the protein. Both contain the opening between helices F and G that provides the primary entry point for substrate into the active site and is the region that experiences the largest movement between the open and closed states. P450tcu, however, has more solvent accessible channels that can potentially provide additional access of solvent protons to the active site, which helps to explain why the product forms *in crystallo*.

DISCUSSION

Thus far, P450tcu is the closest homologue to the well-studied P450cam. With ≈86% sequence identity, it is not surprising that P450tcu and P450cam have very similar structures, enzymatic properties, and selectivity for redox partners. Even so, there are striking differences between these proteins. First, there is a large difference in the thermodynamics of camphor binding, which is entropically driven in P450cam with a ΔH of >0 and a $-T\Delta S$ of <0. In P450tcu, $\Delta H < 0$ and there is more of a balance between ΔH and $-T\Delta S$ and thus, camphor binding is favored both enthalpically and entropically.

Related to thermodynamic differences is the slow low- to high-spin conversion when P450tcu binds camphor. One possible model for explaining these differences is provided in Figure 7.

With P450cam binding of camphor, closing of the active site and dehydration of the active site to give the low- to high-spin transition occur simultaneously. With P450tcu, camphor binds to the active site in a rapid process that does not result in a complete low- to high-spin shift followed by a slower change resulting in a conversion to ≈70% high-spin. The possibility that camphor can bind in the active site but not fully displace the iron water ligand has been observed in the crystal structure of another camphor monooxygenase,

CYP101D2.[27] Therefore, in P450cam, ITC measures binding to the active site together with the processes involved in full conversion to the high-spin state while with P450tcu ITC measures binding to the active site prior to the changes required for conversion to the high-spin state. This further suggests that with P450tcu ITC measures primarily the initial substrate–protein interactions ($\Delta H < 0$) together with at least partial desolvation of the substrate and active site ($-T\Delta S < 0$). With P450cam, ITC also includes protein structural changes involved in the low- to high-spin transition. This can help to improve our understanding of why with P450cam $\Delta H > 0$ because included in this ΔH is not only protein–substrate interactions but also displacement of the water ligand ($\Delta H > 0$) together with various protein changes associated with the open to closed transition. These findings, however, are at odds with the generally accepted view that P450cam activity is tightly associated with a full low- to high-spin transition. This clearly is not the case given that P450tcu is very effcient yet the low- to high-spin change is slow on the time scale of catalysis. This simple picture of a fully high-spin P450 as a requirement for effcient catalysis is no longer adequate. We now know, however, that P450cam is far more dynamic than initially thought and samples stable conformational states that result in the formation of a new active site access channel, substantial restructuring of the active site, and *cis/trans* isomerization of prolines 89 and 105,[20,28,29] all of which are influenced by the redox partner. This provides a more complex view of the conformational dynamics under turnover conditions where P450cam is associated with Pdx as opposed to the simple low- spin to high-spin transition of an isolated P450.

One final difference is that we observe product in the P450tcu active site because of X-ray-driven substrate hydroxylation. In contrast, no product has been observed in crystal structures of wild type ferric P450cam in the absence of its redox partner. This means that synchrotron-generated hydrated electrons promote substrate hydroxylation in ferric P450tcu but not in ferric P450cam. Previous studies have shown that the ability to form product in the X-ray beam is associated with a loosening of the active site access channel by weakening or disrupting the Asp251 ion pairs (Figure 1). Disruption of the salt bridges enables solvent protons to more readily access the active site, which, in turn, enables O_2 activation *in crystallo*.[7,13] This implies that P450tcu might experience larger dynamic motions that enable proton access to the active site *in crystallo*. This view is supported by MD simulations, a comparison of crystallographic *B* factors, and the additional solvent channels found in P450tcu that together underscore dynamical differences between these two P450s. In summary, our results show that despite sharing ≈86% sequence identity and nearly identical crystal structures and enzymatic properties, P450tcu and P450cam exhibit substantial differences in physical properties most likely related to differences in conformational dynamics. These results also strengthen the view that P450s must retain a level of flexibility not only consistent with substrate binding and product egress but also to enable the operation of a proton relay network required for O_2 activation.

Supplementary Material

Refer to Web version on PubMed Central for supplementary material.

ACKNOWLEDGMENTS

The authors thank the SSRL and ALS beamline staff for their support during remote X-ray diffraction data collection. The authors also thank Huiying Li and Christine Hardy for reading the manuscript and for helpful suggestions and the San Diego Super Computer Center.

Funding

This work was supported by National Institutes of Health Grants GM131920 (T.L.P.) and ES025767 (I.F.S.).

ABBREVIATIONS

Pdx	ferredoxin redox partner for P450cam
Pdxtcu	ferredoxin redox partner for P450tcu
Arx	ferredoxin redox partner for CYP101D1
ITC	isothermal titration calorimetry

REFERENCES

(1). Poulos TL (2014) Heme enzyme structure and function. Chem. Rev 114, 3919–3962. [PubMed: 24400737]

(2). Lipscomb JD, Sligar SG, Namtvedt MJ, and Gunsalus IC (1976) Autooxidation and hydroxylation reactions of oxygenated cytochrome P-450cam. J. Biol. Chem 251, 1116–1124. [PubMed: 2601]

(3). Hiruma Y, Hass MA, Kikui Y, Liu WM, Olmez B, Skinner SP, Blok A, Kloosterman A, Koteishi H, Lohr F, Schwalbe H, Nojiri M, and Ubbink M (2013) The structure of the cytochrome p450cam-putidaredoxin complex determined by paramagnetic NMR spectroscopy and crystallography. J. Mol. Biol 425, 4353–4365. [PubMed: 23856620]

(4). Tripathi S, Li H, and Poulos TL (2013) Structural basis for effector control and redox partner recognition in cytochrome P450. Science 340, 1227–1230. [PubMed: 23744947]

(5). Lee YT, Wilson RF, Rupniewski I, and Goodin DB (2010) P450cam visits an open conformation in the absence of substrate. Biochemistry 49, 3412–3419. [PubMed: 20297780]

(6). Liou SH, Mahomed M, Lee YT, and Goodin DB (2016) Effector Roles of Putidaredoxin on Cytochrome P450cam Conformational States. J. Am. Chem. Soc 138, 10163–10172. [PubMed: 27452076]

(7). Batabyal D, and Poulos TL (2013) Crystal structures and functional characterization of wild-type CYP101D1 and its active site mutants. Biochemistry 52, 8898–8906. [PubMed: 24261604]

(8). Yang W, Bell SG, Wang H, Zhou W, Hoskins N, Dale A, Bartlam M, Wong LL, and Rao Z (2010) Molecular characterization of a class I P450 electron transfer system from Novosphingobium aromaticivorans DSM12444. J. Biol. Chem 285, 27372–27384. [PubMed: 20576606]

(9). Tsang HL, Huang JL, Lin YH, Huang KF, Lu PL, Lin GH, Khine AA, Hu A, and Chen HP (2016) Borneol Dehydrogenase from Pseudomonas sp. Strain TCU-HL1 Catalyzes the Oxidation of (+)-Borneol and Its Isomers to Camphor. Appl. Environ. Microbiol 82, 6378–6385. [PubMed: 27542933]

(10). Sevrioukova IF, Li H, and Poulos TL (2004) Crystal structure of putidaredoxin reductase from Pseudomonas putida, the final structural component of the cytochrome P450cam monooxygenase. J. Mol. Biol. 336, 889–902. [PubMed: 15095867]

(11). Sevrioukova IF, Hazzard JT, Tollin G, and Poulos TL (2001) Laser flash induced electron transfer in P450cam monooxygenase: putidaredoxin reductase-putidaredoxin interaction. Biochemistry 40, 10592–10600. [PubMed: 11524002]

(12). Churbanova IY, Poulos TL, and Sevrioukova IF (2010) Production and characterization of a functional putidaredoxin reductase-putidaredoxin covalent complex. Biochemistry 49, 58–67. [PubMed: 19954240]

(13). Batabyal D, Richards LS, and Poulos TL (2017) Effect of Redox Partner Binding on Cytochrome P450 Conformational Dynamics. J. Am. Chem. Soc 139, 13193–13199. [PubMed: 28823160]

(14). Battye TG, Kontogiannis L, Johnson O, Powell HR, and Leslie AG (2011) iMOSFLM: a new graphical interface for diffraction-image processing with MOSFLM. Acta Crystallogr., Sect. D: Biol. Crystallogr 67, 271–281. [PubMed: 21460445]

(15). Kabsch W (2010) Xds. Acta Crystallogr., Sect. D: Biol. Crystallogr 66, 125–132. [PubMed: 20124692]

(16). Winn MD, Ballard CC, Cowtan KD, Dodson EJ, Emsley P, Evans PR, Keegan RM, Krissinel EB, Leslie AG, McCoy A, McNicholas SJ, Murshudov GN, Pannu NS, Potterton EA, Powell HR, Read RJ, Vagin A, and Wilson KS (2011) Overview of the CCP4 suite and current developments. Acta Crystallogr., Sect. D: Biol. Crystallogr 67, 235–242. [PubMed: 21460441]

(17). McCoy AJ, Grosse-Kunstleve RW, Adams PD, Winn MD, Storoni LC, and Read RJ (2007) Phaser crystallographic software. J. Appl. Crystallogr 40, 658–674. [PubMed: 19461840]

(18). Adams PD, Afonine PV, Bunkoczi G, Chen VB, Echols N, Headd JJ, Hung LW, Jain S, Kapral GJ, Grosse Kunstleve RW, McCoy AJ, Moriarty NW, Oeffner RD, Read RJ, Richardson DC, Richardson JS, Terwilliger TC, and Zwart PH (2011) The Phenix software for automated determination of macromolecular structures. Methods 55, 94–106. [PubMed: 21821126]

(19). Hollingsworth SA, and Poulos TL (2015) Molecular dynamics of the P450cam-Pdx complex reveals complex stability and novel interface contacts. Protein Sci. 24, 49–57. [PubMed: 25307478]

(20). Follmer AH, Mahomed M, Goodin DB, and Poulos TL (2018) Substrate-Dependent Allosteric Regulation in Cytochrome P450cam (CYP101A1). J. Am. Chem. Soc 140, 16222–16228. [PubMed: 30376314]

(21). Roe DR, and Cheatham TE 3rd (2013) PTRAJ and CPPTRAJ: Software for Processing and Analysis of Molecular Dynamics Trajectory Data. J. Chem. Theory Comput 9, 3084–3095. [PubMed: 26583988]

(22). Hollingsworth SA, Batabyal D, Nguyen BD, and Poulos TL (2016) Conformational selectivity in cytochrome P450 redox partner interactions. Proc. Natl. Acad. Sci. U. S. A 113, 8723–8728. [PubMed: 27439869]

(23). Glascock MC, Ballou DP, and Dawson JH (2005) Direct observation of a novel perturbed oxyferrous catalytic intermediate during reduced putidaredoxin-initiated turnover of cytochrome P-450-CAM: probing the effector role of putidaredoxin in catalysis. J. Biol. Chem 280, 42134–42141. [PubMed: 16115886]

(24). Kuznetsov VY, Poulos TL, and Sevrioukova IF (2006) Putidaredoxin-to-cytochrome P450cam electron transfer: differences between the two reductive steps required for catalysis. Biochemistry 45, 11934–11944. [PubMed: 17002293]

(25). Sligar SG, Debrunner PG, Lipscomb JD, Namtvedt MJ, and Gunsalus IC (1974) A role of the putidaredoxin COOH-terminus in P-450cam (cytochrome m) hydroxylations. Proc. Natl. Acad. Sci. U. S. A 71, 3906–3910. [PubMed: 4530269]

(26). Li H, Narasimhulu S, Havran LM, Winkler JD, and Poulos TL (1995) Crystal Structure of Cytochrome P450cam Complexed with Its Catalytic Product, 5-exo-Hydroxycamphor. J. Am. Chem. Soc 117, 6297–6299.

(27). Yang W, Bell SG, Wang H, Zhou W, Bartlam M, Wong L-L, and Rao Z (2011) The structure of CYP101D2 unveils a potential path for substrate entry into the active site. Biochem. J 433, 85–93. [PubMed: 20950270]

(28). Follmer AH, Tripathi S, and Poulos TL (2019) Ligand and Redox Partner Binding Generates a New Conformational State in Cytochrome P450cam (CYP101A1). J. Am. Chem. Soc 141, 2678–2683. [PubMed: 30672701]

(29). OuYang B, Pochapsky SS, Dang M, and Pochapsky TC (2008) A functional proline switch in cytochrome P450cam. Structure 16, 916–923. [PubMed: 18513977]

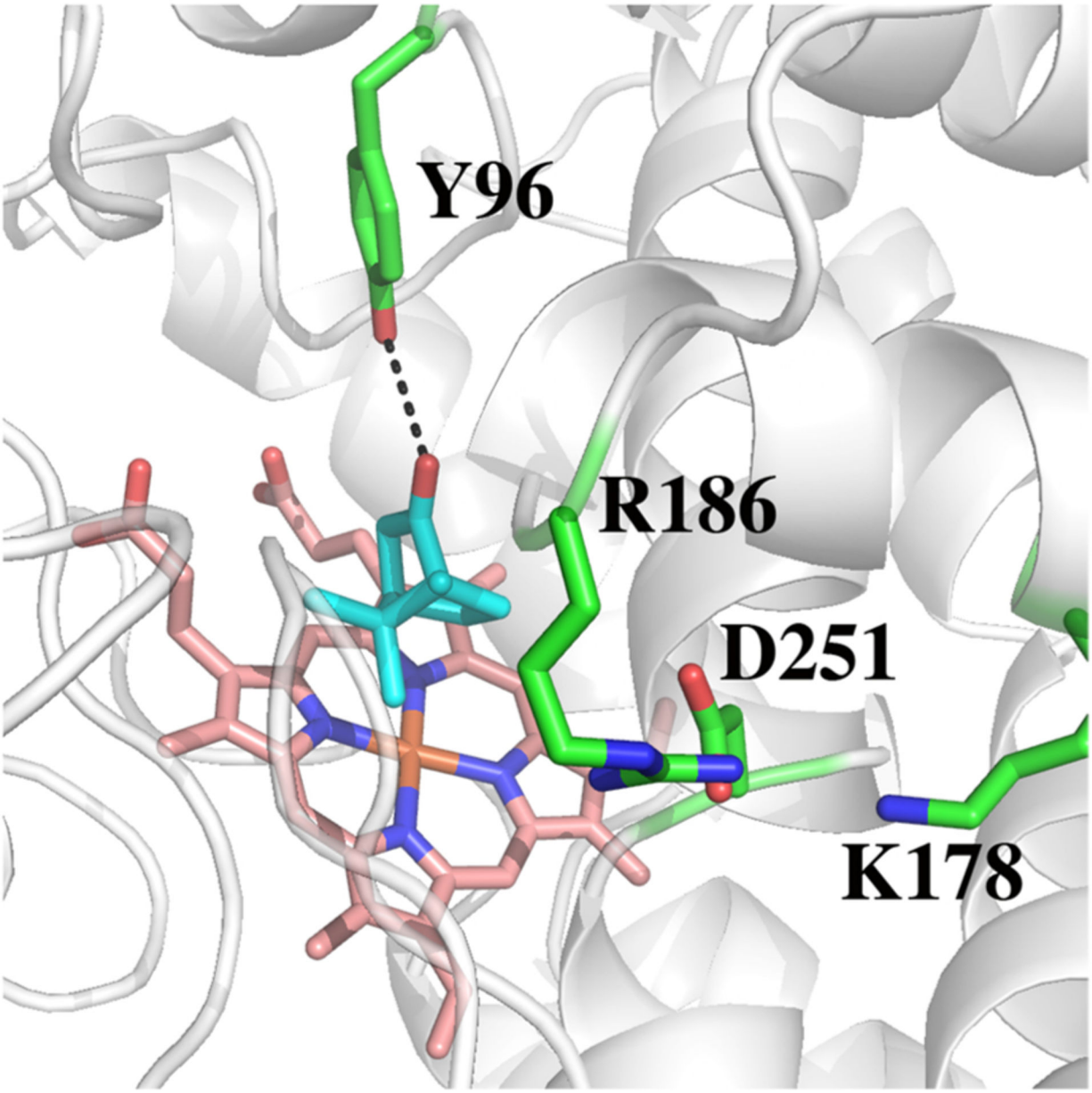

Figure 1.

Active site of P450cam highlighting the salt bridges among Asp251, Arg186, and Lys178. CYP101D1 is very similar except the homologue to Lys178 is a Gly.

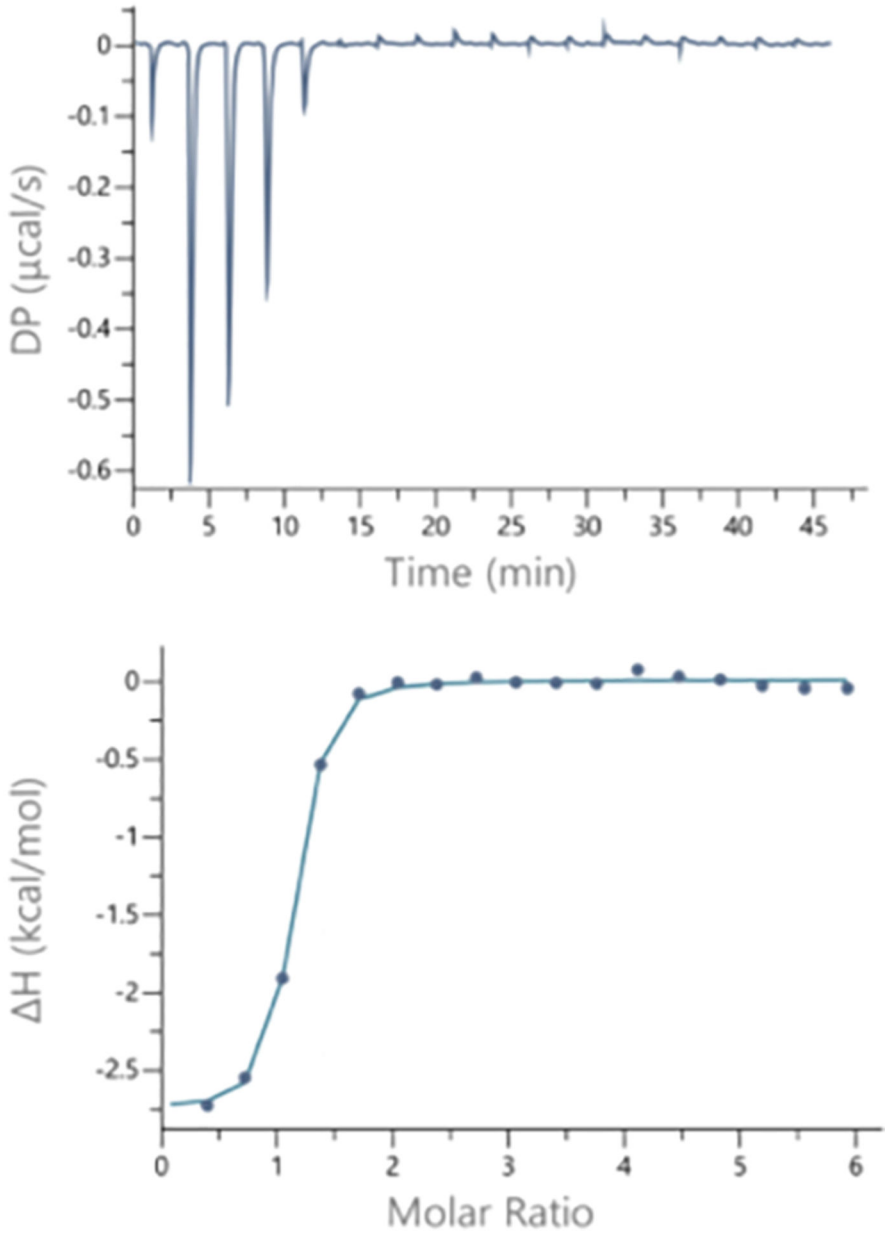

Figure 2.
Isothermal titration calorimetry of camphor binding to P450tcu.

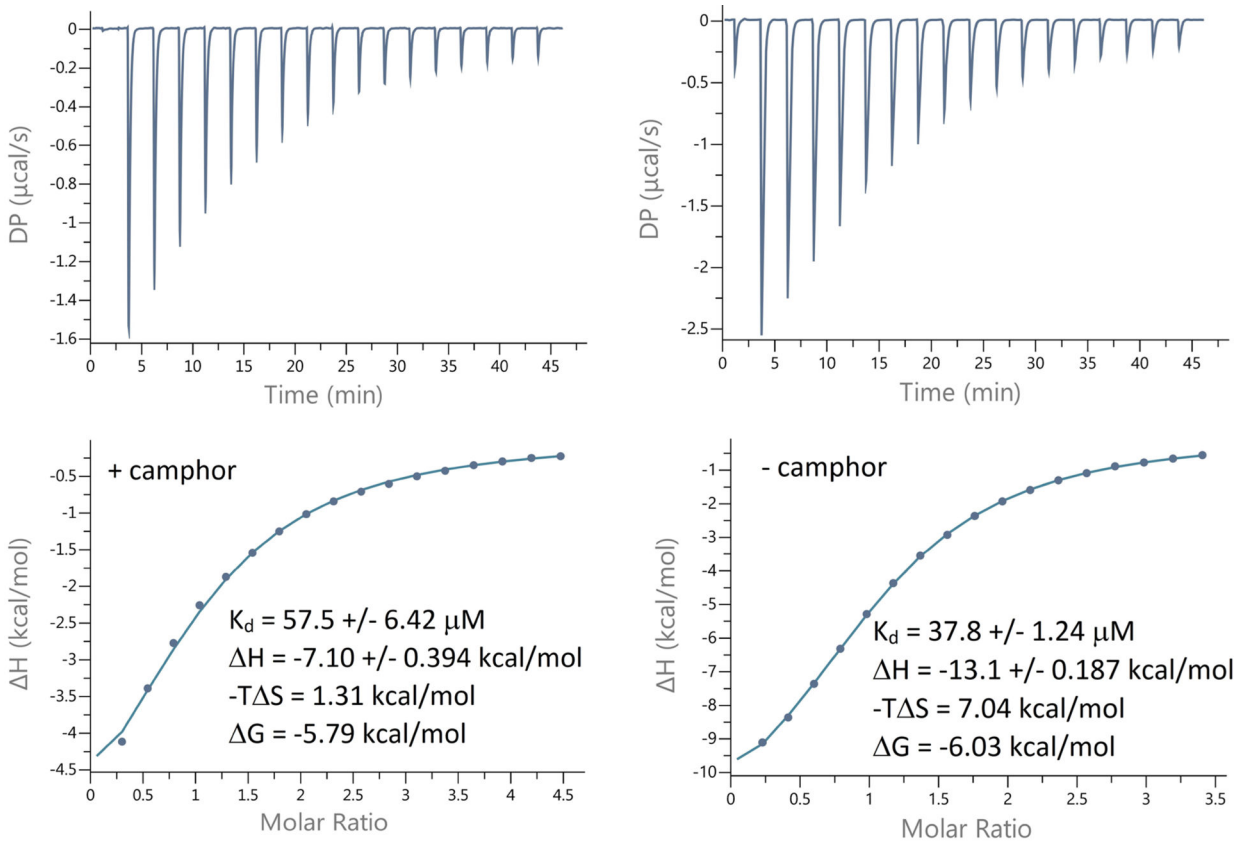

Figure 3.

ITC thermograms for Pdxtcu binding to P450tcu measured in the presence and absence of D-camphor. Similar to the P450cam-Pdx pair, Pdxtcu has a higher binding affinity for an open (or substrate-free) form of P450tcu.

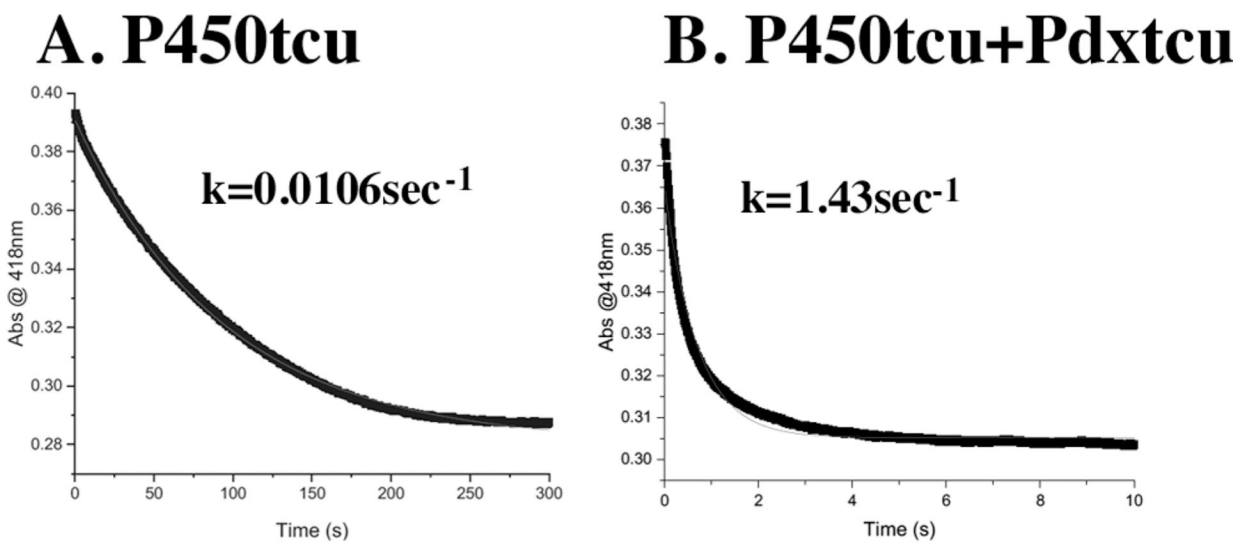

Figure 4.

Decomposition of the P450tcu-oxy complex in the presence and absence of 2 equiv of Pdxtcu. Similar to the P450cam-Pdx redox pair,[23] the binding of oxidized Pdxtcu substantially increases the rate of decay of the P450tcu-oxy complex.

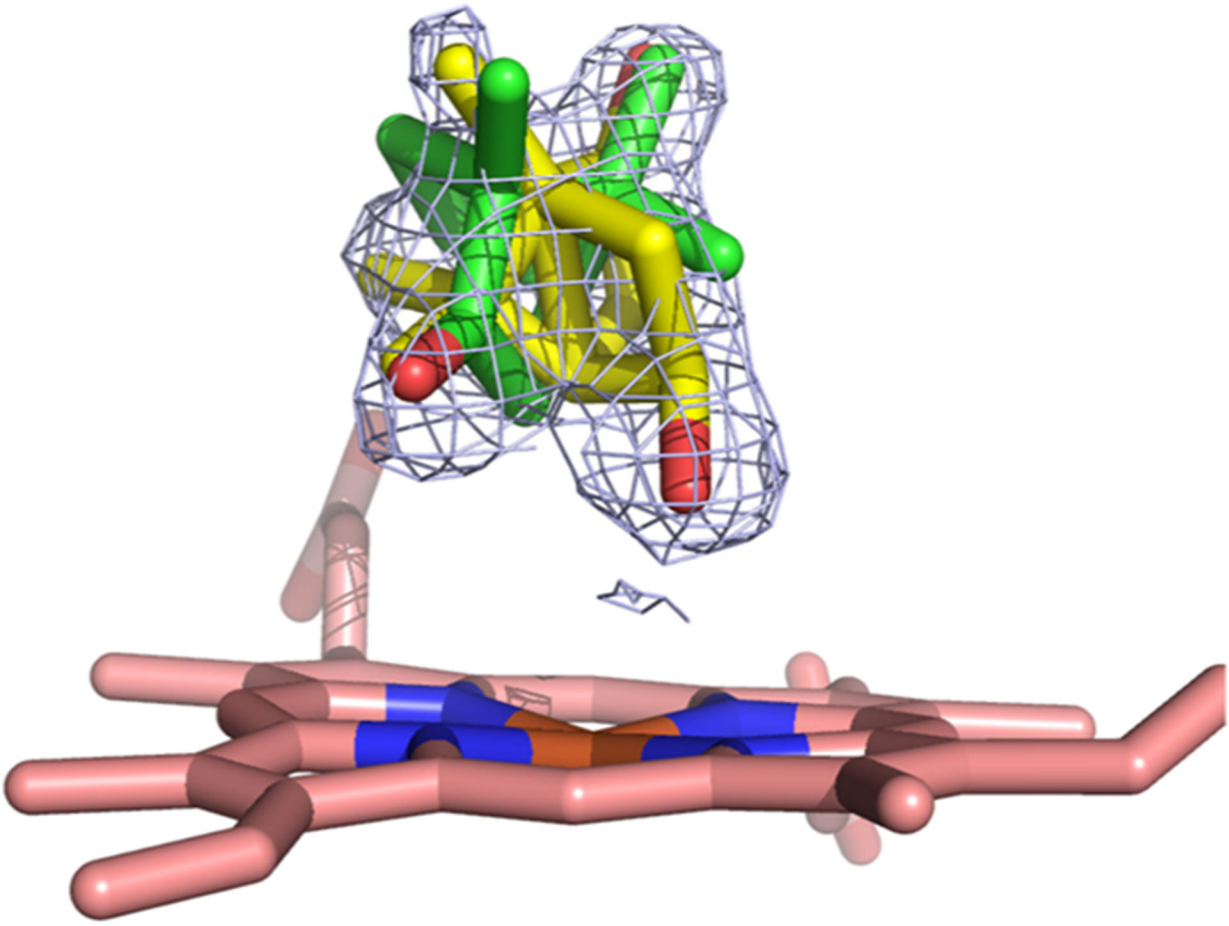

Figure 5.

$2F_o - F_c$ electron density map contoured at 1.0σ. The density is consistent with a product molecule occupying two different orientations. The yellow molecule is in the productive binding mode.

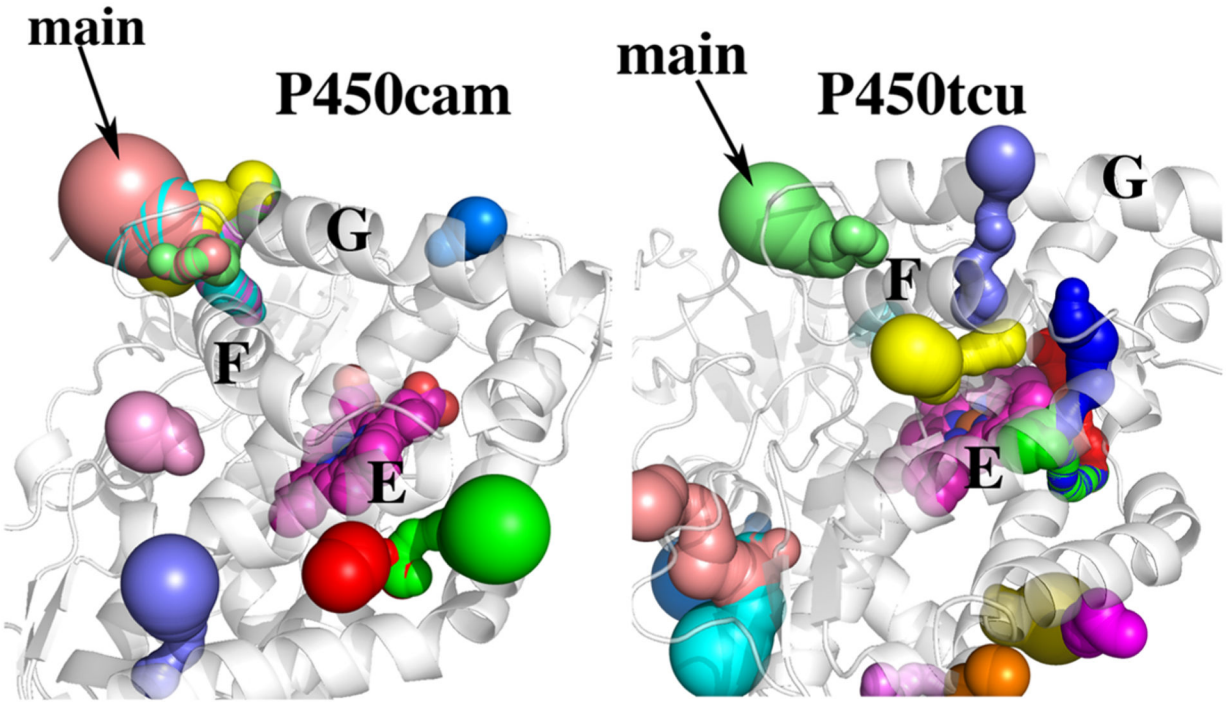

Figure 6.

Solvent access channels found by Mole2 in P450cam and P450tcu. The colored tubes represent channels that can be accessed by a solvent probe. Both contain the same main access channels between helices F and G. P450tcu, however, has more channels connecting the surface to the active site.

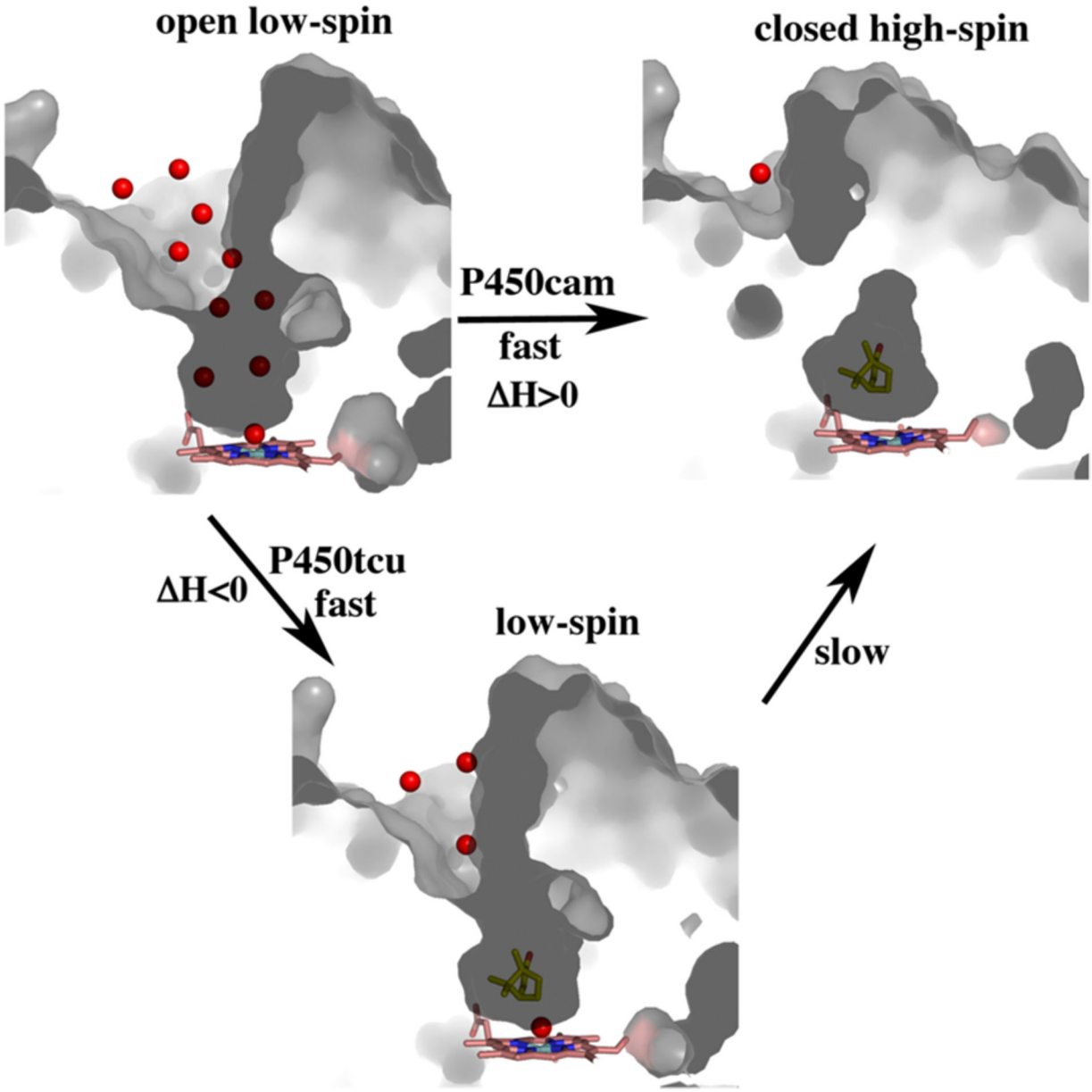

Figure 7.

Possible model for the binding of camphor to P450cam and P450tcu. The models are surface representations of the open, closed, and intermediate states with the camphor as yellow sticks and water molecules as red spheres, one of which is coordinated to the heme iron. In P450cam, camphor binds to the active site, resulting in a rapid low- to high-spin transition and desolvation of the active site. This is the process measured by ITC giving a ΔH of >0. In P450tcu, ITC measures an initial rapid binding to the open form possibly resulting in a partially closed state giving a mix of low- and high-spin states. This is followed by a slow transition to the closed high-spin state observed in the crystal structure.

Table 1.

Isothermal Titration Calorimetry of Substrate Binding to P450cam and P450tcu

	ΔH (kcal/mol)	−TΔS (kcal/mol)	ΔG (kcal/mol)	K_D (μM)
P450cam[a]	2.13 ± 0.09	−10.2	−8.09	1.2 ± 0.4
P450tcu	−2.77 ± 0.04	−5.63	−8.40	0.702 ± 0.098

[a]From ref 13.

Table 2.

Enzymatic Characterization of P450tcu[a]

enzyme	redox partner	k_{cat} (min^{-1})	% coupling efficiency
P450tcu	Pdx	758 ± 30	~93
P450tcu	Pdxtcu	624 ± 13	~9S
P450cam	Pdx	913 ± 20	~95
P450cam	Pdxtcu	621 ± 21	~9S
P450tcu	Arx	ND[b]	ND[b]
P450tcu	PdxΔ106	ND[b]	ND[b]

[a] k_{cat} was determined by the rate of NADH oxidation. The % coupling efficiency is the ratio of NADH oxidized to product formed. Pdx is the native redox partner for P450cam, while Pdxtcu is the native redox partner for P450tcu. Arx is the redox partner for CYP101D1, and PdxΔ106 is Pdx with the C-terminal Trp106 removed. Pdr is the native reductase of P450cam and was used for all of the reactions.

[b] Not detectable.

Table 3.

B Factors (Å^2) Computed from MD Simulations[a]

	camphor	Tyr96	Asp251
P450cam	55.5	22.2	10.5
P450tcu	73.9	61.9	19.4

[a] *B* factors were computed using 50000 snapshots obtained from ten 100 ns MD runs.